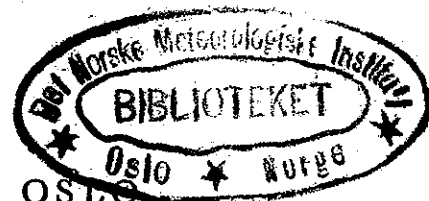


X  
DET NORSKE VIDENSKAPS-AKADEMI I OSLO



**GEOFYSISKE PUBLIKASJONER**  
**GEOPHYSICA NORVEGICA**

*Bill. Hovel.*  
*els.*  
*(=els. 1)*

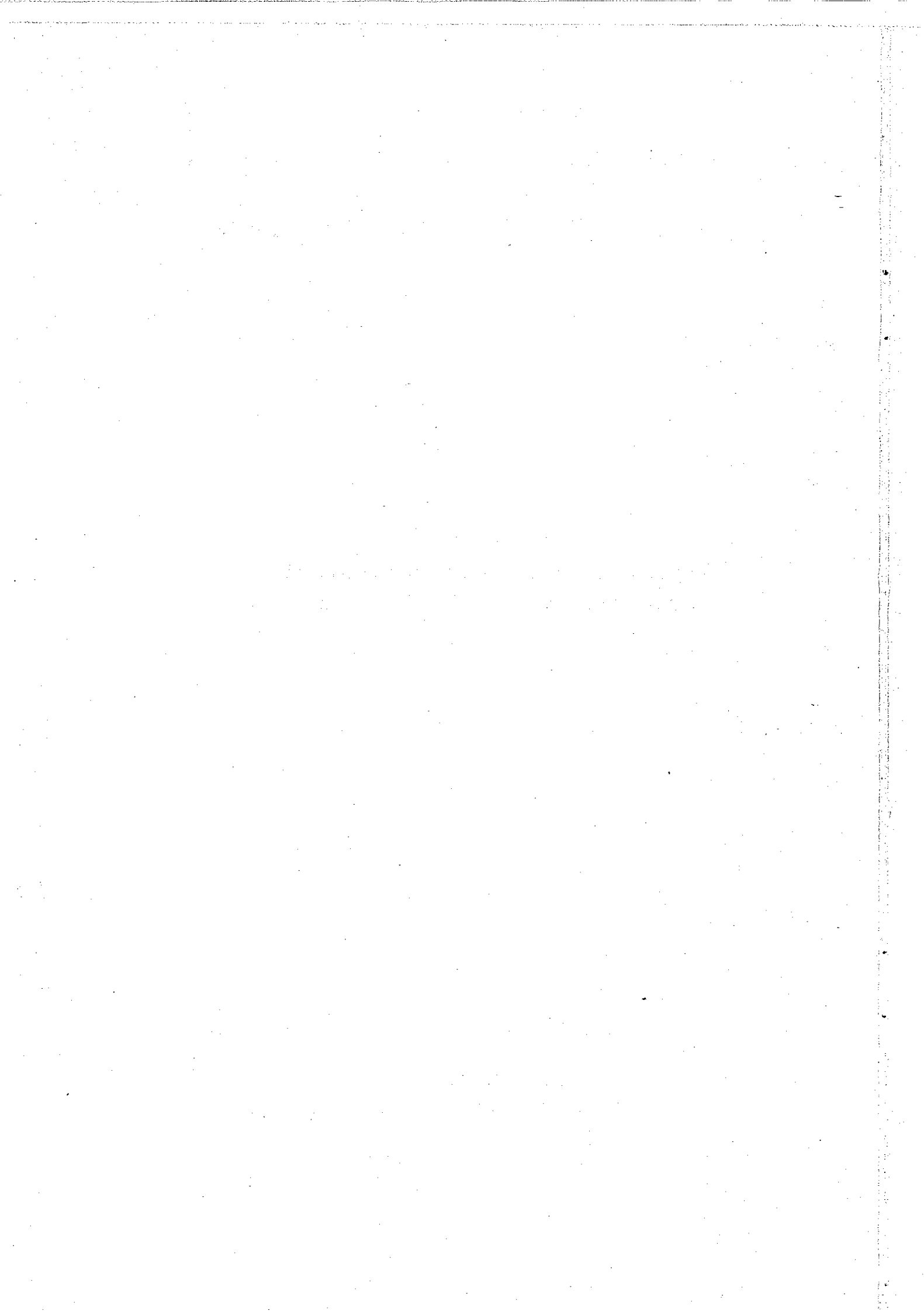
Vol. XXIII. Nr. 2

January 1962

BERNT MÆHLUM

Small scale structure and drift in the sporadic  
*E* layer as observed in the auroral zone

OSLO 1962  
OSLO UNIVERSITY PRESS



G E O F Y S I S K E P U B L I K A S J O N E R  
G E O P H Y S I C A N O R V E G I C A

VOL. XXIII

NO 2.

SMALL SCALE STRUCTURE AND DRIFT IN THE SPORADIC  
E LAYER AS OBSERVED IN THE AURORAL ZONE

BY BERNT MÆHLUM

FREMLAGT I VIDENSKAPS-AKADEMIETS MØTE DEN 10DE MARS 1961 AV HARANG

**Summary.** Results from a study of the fading pattern of the *Es* echo in the auroral zone are presented. The irregularities in the fading pattern are clearly elongated in an east/west direction, and the mean meridional extent of the irregularities is 250 m. The irregularities drift towards the east or the south-west, and velocities as high as  $1450 \text{ m sec}^{-1}$  have been observed.

The observations are discussed in a semiquantitative way in the light of existing theories of auroral ionization.

**1. Introduction.** The ionization in the sporadic *E* layer is known to occur in "patches" with smaller "clouds" of ionization embedded. In the present paper the former will be referred to as the "large scale" structure, while the latter will be called the "small scale" structure. Studies of the "large scale" structure, based upon the time variations of the maximum plasma frequency of the layer for multi-station observations, indicate that the mean horizontal extent of the "patches" at the middle latitudes is of the order of 200 km (GERSON [1] and RAWER [2]), or more (OKSMAN and BOWHILL [3]). In the auroral zone the corresponding distance seems to be much larger, at least during geomagnetically quiet periods (MÆHLUM [4]).

The drift speed of the "large scale" irregularities in the sporadic *E* layer vary from 30 to  $130 \text{ m sec}^{-1}$  at middle latitudes (GERSON [1]), while the drift speed in the auroral zone is somewhat higher (HAGG and HANSSON [5]).

Studies of the "small scale" irregularities in the sporadic *E* region have been performed by BRIGGS [6] in England and by WRIGHT [7] near the equator (Ibadan). In the present paper results will be given from a study of the "small scale" irregularities in the night-time *Es* region of the auroral ionosphere. The study is based on observations made at Tromsø during 1958 and 1959.

The method used is briefly described in Section 2, and results from the study are given in Sections 3, 4 and 5. The possible physical processes involved in the formation and drift of the small scale irregularities are discussed in Section 6.

**2. Method of observation.** The mean structure and movement of the amplitude pattern over the ground may be obtained by a method introduced by the Radio Section at the Cavendish Laboratory in Cambridge, England [8—11]. The calculation is based upon the time variation of the echo amplitude at three closely spaced receivers.

In order to deduce the structure and drift of the amplitude pattern of the sporadic *E* echo from the time variation of the echo amplitude at the three points, the following assumptions have been made [10—11]:

- 1) The curves of constant spatial autocorrelation are conformal, concentric ellipses.
- 2) The amplitude pattern changes very slowly as it moves.
- 3) The temporal autocorrelation function is conformal to the spatial, one-dimensional autocorrelation function.

With these assumptions the spatial and temporal autocorrelation functions of the echo amplitude may be deduced, and from these the mean structure and drift of the amplitude pattern of the echo may be obtained. A detailed description of the method of analysis is given in an Appendix.

A pulsed transmitter with a repetition frequency of 50 cps and a pulse duration of 150  $\mu$ sec was used during the observations, and the transmitted peak power was approximately 7 kW. The signals were received at the three antennas arranged in a right-angled triangle (Vide Fig. (A1)), and the separation between the center (B) and the west (C) or the south (A) antenna was 130 meters. The signals were fed through three receivers to a three-beam cathode ray oscilloscope.

It was found that the reflected wave often consisted of more than one component, and that the different components showed different fading. By using a gate technique, however, it was normally possible to separate one of the components only. The echoes were recorded on photographic paper at a speed of 1 cm sec<sup>-1</sup>. The records were time marked each 8 sec. A detailed description of the equipment used has been given by HARANG and PEDERSEN [12].

Frequencies between 2.0 and 2.65 Mc sec<sup>-1</sup> were used in the observations. A typical fading record is given in Fig. 1. This illustration shows that the correlation is much higher in the east/west direction than in the north/south direction. This point will be more fully treated in the following sections.

Due to the high noise level and interference caused by radio stations, more than 60 % of the records was not suitable for further analysis. Furthermore, records obtained during conditions when the echo was very spread and showed rapid fading could not be used. In order to obtain a significant autocorrelation function, only periods when the fading rate was less than 2 cps were selected. Thus only a small percentage of the records could be analysed in detail.

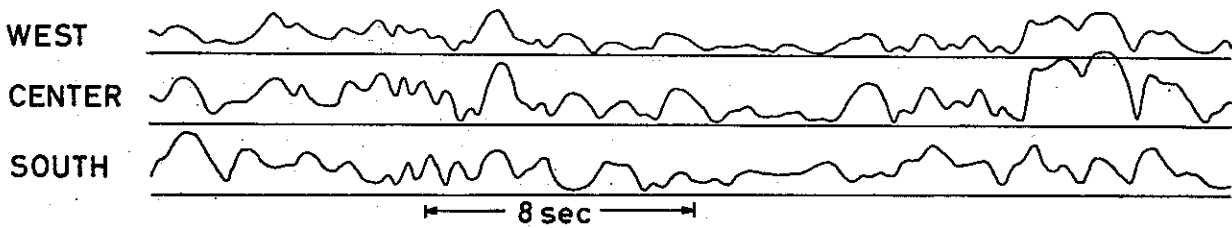


Fig. 1. Typical record showing the fading of the *Es* echo at three closely spaced receivers.

**3. Structure of the amplitude pattern of the Sporadic E echo.** The sporadic *E* echo as observed in Tromsø is often spread during the early evening hours, and the fading rate is of the order of 1.5 cps. Towards midnight the echo normally becomes less spread and the fading rate decreases. The low fading rate, sometimes less than 0.2 cps, is associated with a blanketing *Es* layer, which gives several multiple reflections, or the retardation type of *Es*. There is a clear positive correlation between the equivalent height of reflection and the fading rate, as shown in Table (1) for a typical night.

Approximately 40 samples, varying in length from 25 to 60 seconds, were selected for further analysis, and the amplitude was read at each 1/10 of a second.

Table 1. Time variation of the fading rate (cps) and the equivalent height of reflection (km) 17–18 July 1958.

Time	Height of reflection	Fading rate
2100	150	0,65
2115	150	0,49
2130	190	2,10
2215	200	2,13
2230	100	0,11
2300	105	0,16
2315	115	0,41
2330	95	0,14
0130	100	0,18

The mean structure and drift of the amplitude pattern were deduced by the "Cambridge method" (given in the Appendix). According to this method the curves of constant spatial autocorrelation are assumed to be concentric, conformal ellipses. The "correlation ellipses" are thus a measure of the mean size and shape of the irregularities in the amplitude pattern. Correlation ellipses deduced for 10 sample records are shown in Fig. (2) (arbitrary scale). The drift velocities deduced for the same samples are indicated by arrows.

No seasonal variation in the axis ratio nor the orientation could be traced. Results from the study are given in Fig. (3), in which the orientation of the major axis

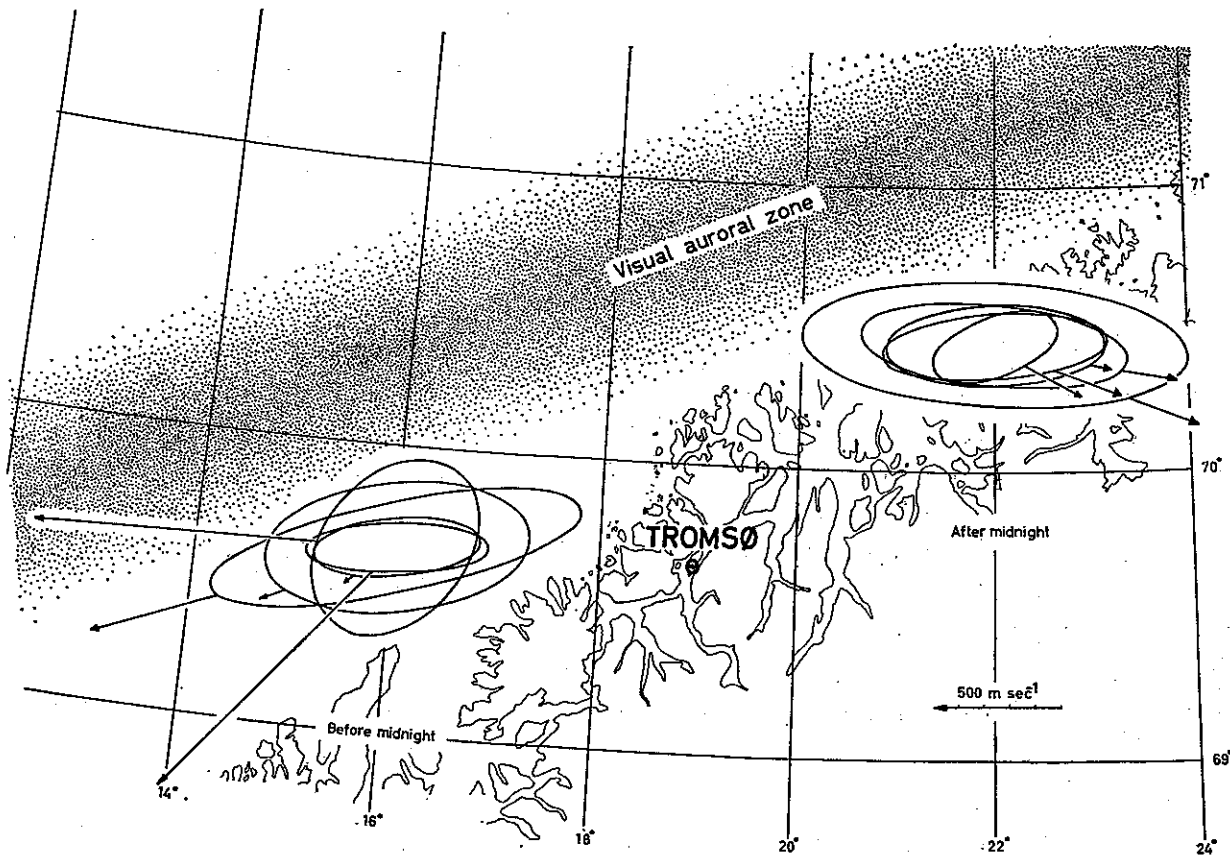


Fig. 2. Examples of the correlation ellipses and drift velocities of the *Es* amplitude pattern.

of the correlation ellipses is plotted versus the axis ratio. The axis ratios vary from 1.2 to 7.8, and the mean value is approximately 3.0.

It is obvious from Fig. (3) that the great majority of the *Es* echo amplitude patterns consists of irregularities which are slightly elongated in an east/west direction. The observed distribution of the orientations of the major axis is given in Fig. (4). We realize that 60 % of the correlation ellipses is orientated with their major axis in directions which are less than  $10^\circ$  off the east/west direction.

The "small scale" structure of the amplitude pattern of the sporadic *E* echo shows a peculiar variation with latitude. Near the equator the irregularities in the pattern are highly stretched in the north/south direction (WRIGHT [7]), whereas observations at middle latitudes ( $55^\circ$  geom lat) indicate an isometric *Es* amplitude pattern (BRIGGS [6]). As the sporadic *E* layer at middle and low latitudes most certainly is not of the same origin as the sporadic *E* layer in the auroral zone, these results are not relevant to the observations obtained at Tromsø. The structure of the night-time *Es* layer has, however, been studied by HARANG and PEDERSEN [12] at Kjeller ( $60^\circ$  geom lat). From a statistical study of the time shifts between "similar fades", as observed at three closely spaced receivers, these authors argue that the irregularities in the amplitude pattern of the *Es* echo at Kjeller are elongated in a north/south direction. In the present paper

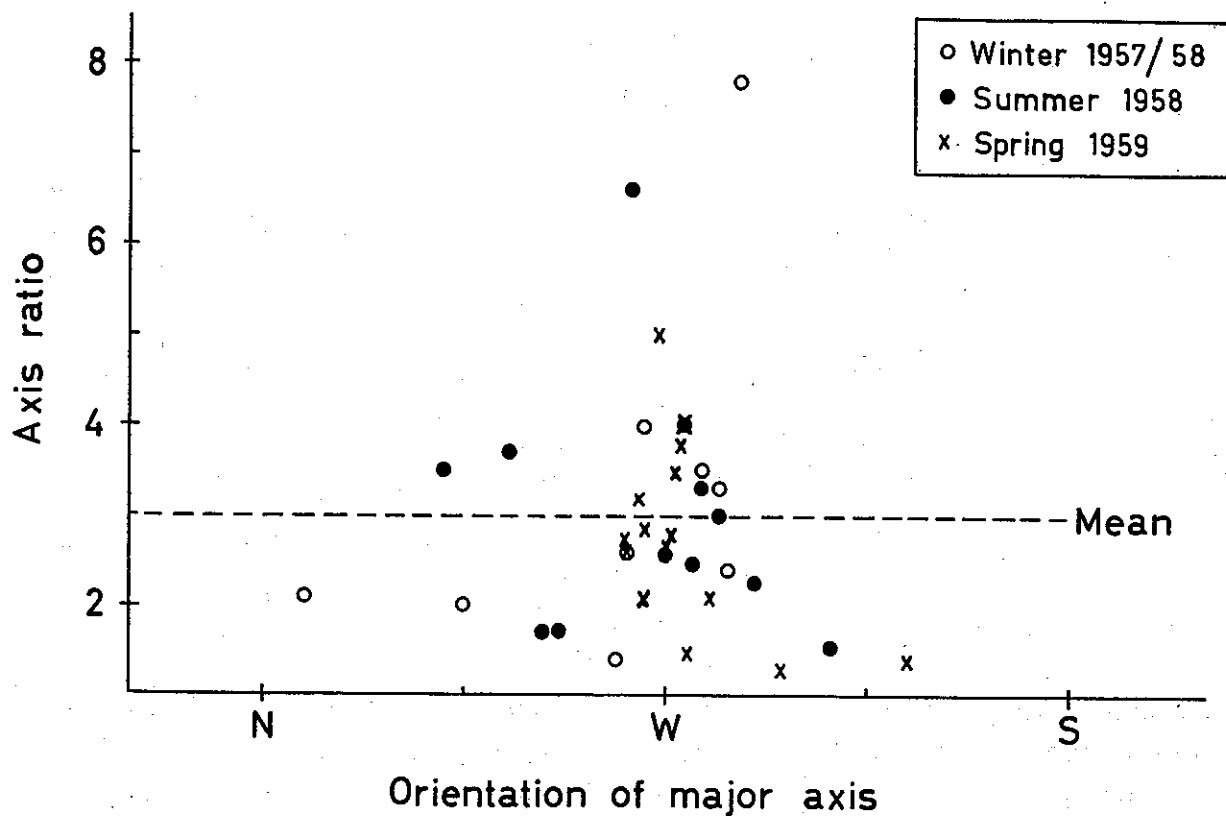


Fig. 3. The axis ratio of the "correlation ellipses" of the amplitude pattern of the *E<sub>s</sub>* echo plotted versus the orientation of the major axis.

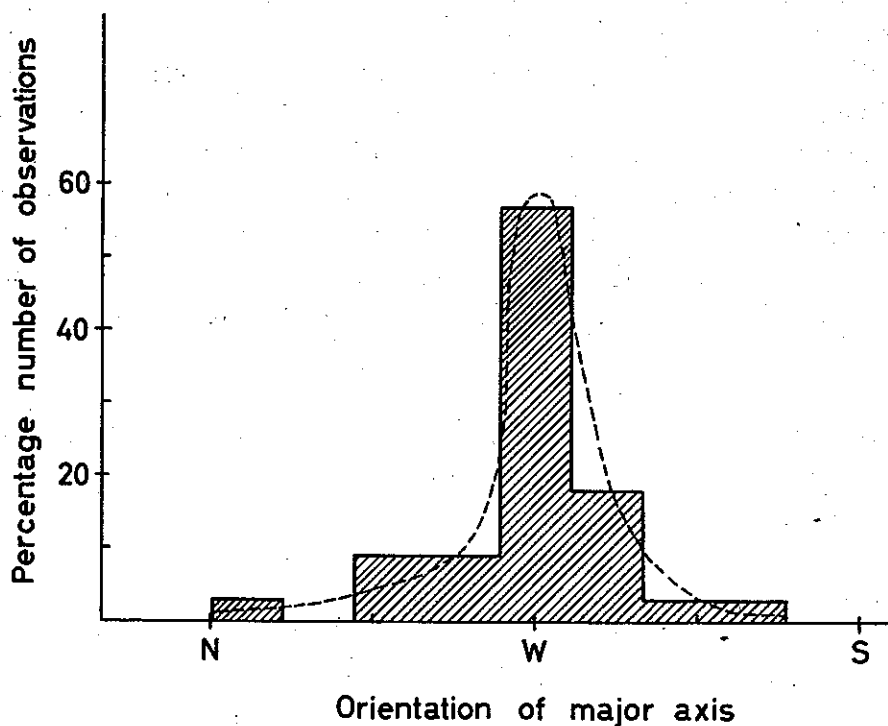


Fig. 4. Distribution of the orientation of the major axis in the "correlation ellipses".

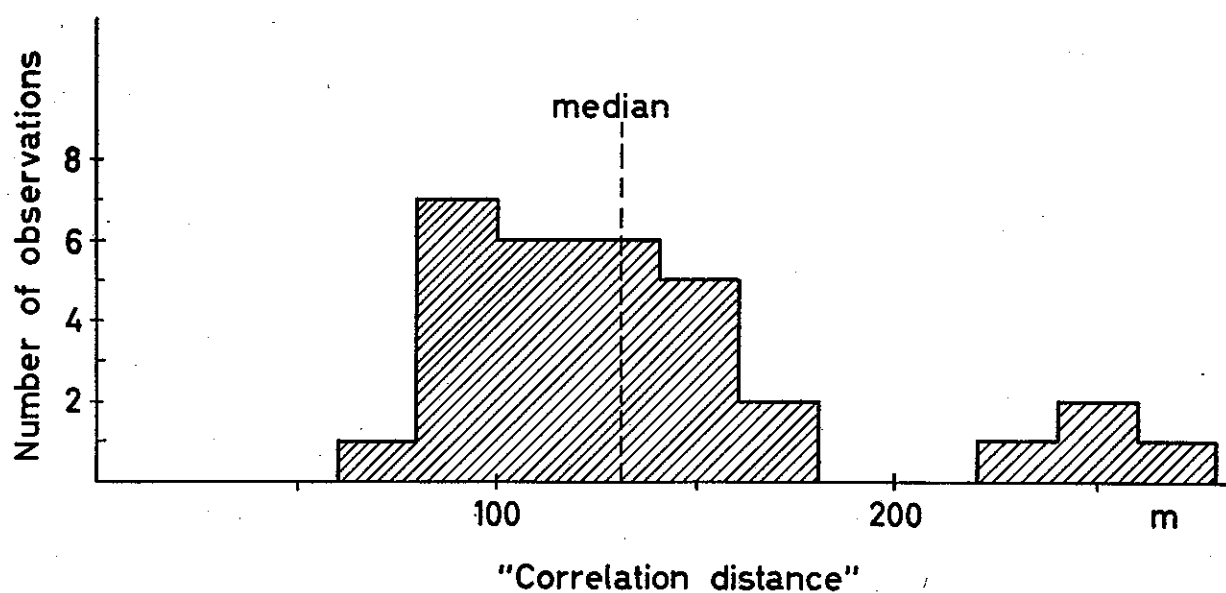


Fig. 5. Distribution of the correlation distance.

we have no explanation to offer for the apparent discrepancy between the small scale structure of the night-time *Es* amplitude pattern observed at Kjeller and that observed at Tromsø. The geometry of the earth's magnetic field may possibly be of some importance. This has, however, not been investigated in details.

Let the "correlation distance" be defined as the minor semiaxis in the ellipse of constant spatial correlation equal to 0.5. This "correlation distance" may, together with the axis ratio of the ellipse, serve as a measure of the mean horizontal extent of the irregularities in the amplitude pattern. The "correlation distance" varies from 60 to 270 m, and the mean value is approximately 130 m (Vide Fig. (5)).

No significant variation of the correlation distance with magnetic activity could be traced. This result is somewhat unexpected, as the ionosonde records clearly show that the *Es* types observed at Tromsø change from geomagnetically quiet to disturbed conditions. During quiet conditions the retardation type of *Es* is most frequently observed, whereas the non-retardation types predominate during disturbed conditions (MÆHLUM [4]).

**4. Movement of the amplitude pattern of the *Es*-echo.** The *true drift* of the amplitude pattern of the sporadic *E* echo, as defined in the Appendix, has been deduced for 40 sample records. The observed distribution of the drift speeds is given in Fig. (6). Approximately 65% of the velocities is less than  $400 \text{ m sec}^{-1}$ , about 5% of the observations exceeds  $1200 \text{ m sec}^{-1}$ , and the median is  $280 \text{ m sec}^{-1}$ .

The drift of the amplitude pattern is usually assumed to be twice the velocity of the ionospheric drift. The mean drift speed of the irregularities in the ionospheric *Es*-layer in the auroral zone is therefore of the order  $150 \text{ m sec}^{-1}$ . This value is somewhat higher than the sporadic *E* layer drift speeds observed at middle latitude stations



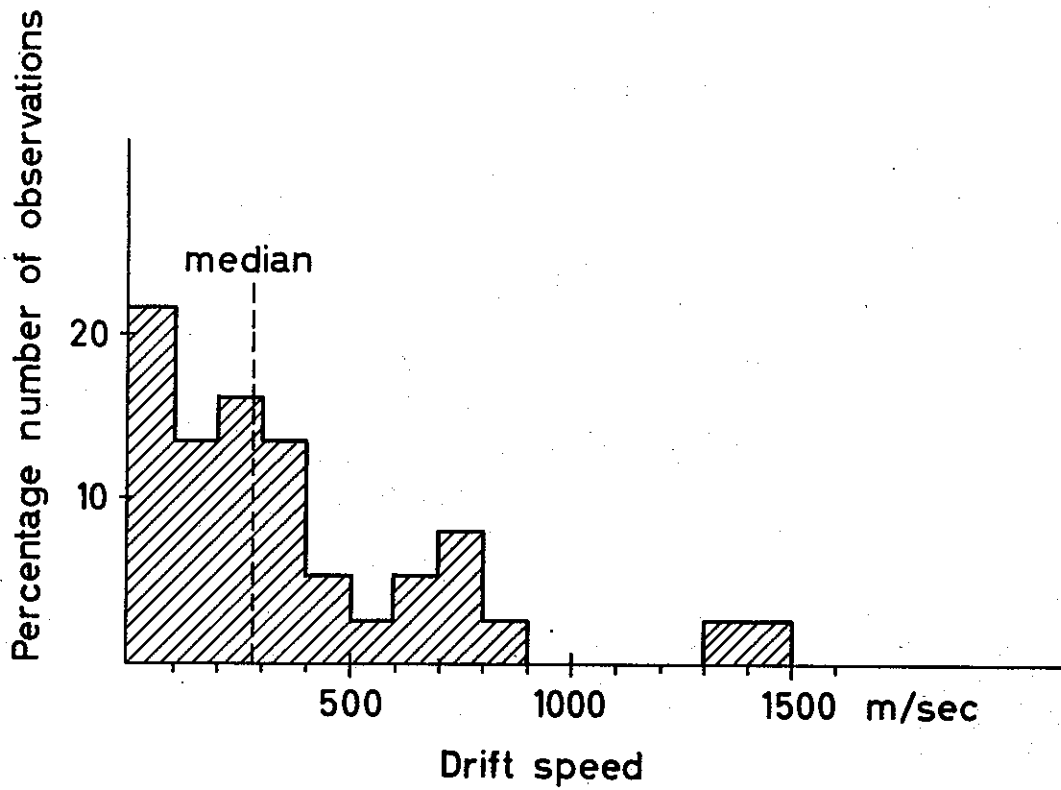


Fig. 6. Distribution of the drift speed of the amplitude patterns of the *Es* echo at Tromsø.

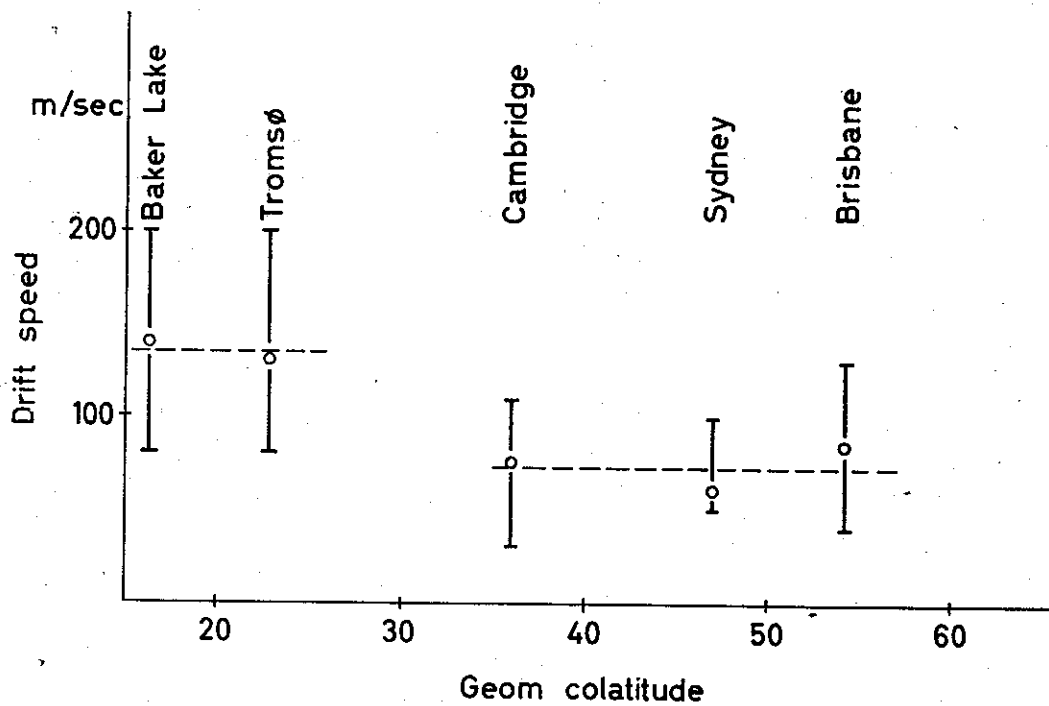


Fig. 7. Latitude variation of the mean drift speed of the sporadic *E* layer.

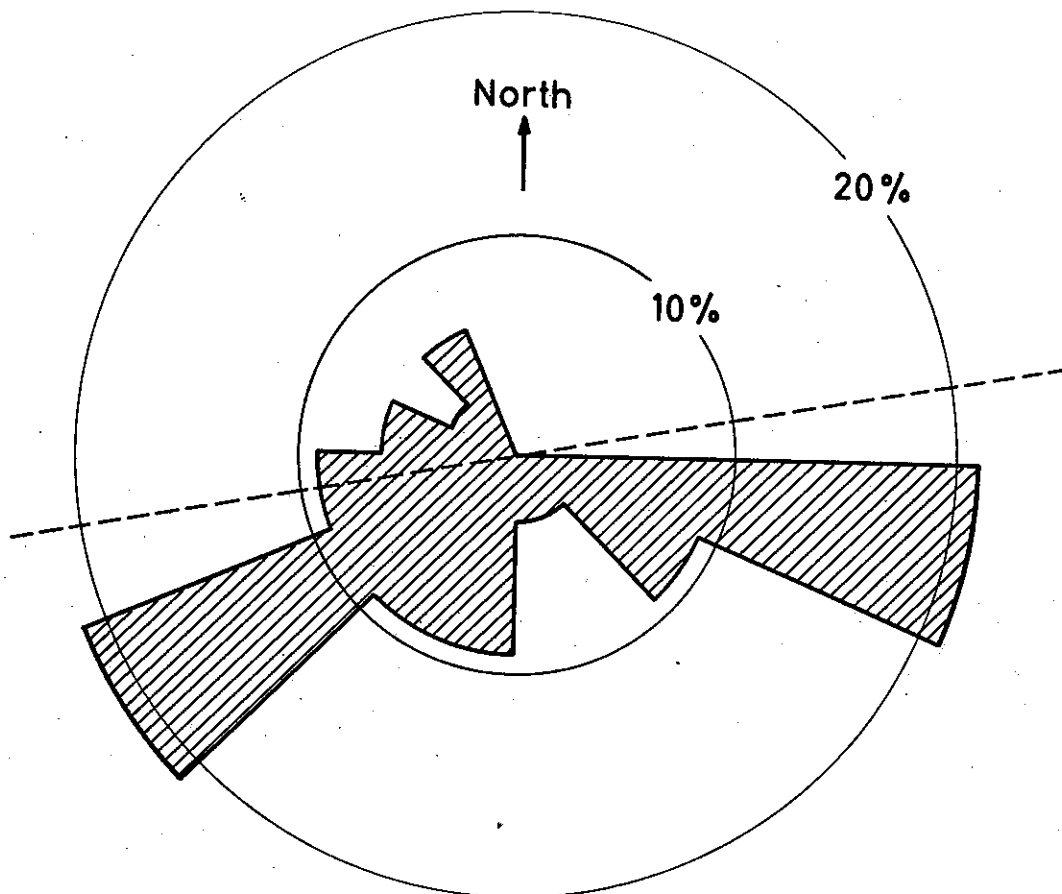


Fig. 8. Distribution of the observed drift directions of the  $E_s$  amplitude pattern at Tromsø (polar plot). The visual auroral zone is indicated by the broken line.

[13, 14 and 15], being approximately  $70 \text{ m sec}^{-1}$ . The latitudinal variation of the drift speed in the sporadic  $E$  layer is shown in Fig. (7). The drift velocities observed at Tromsø are consistent with drift observations at Canadian stations (MEEK [16]). It is, however, emphasized that the results given in Fig. (7) have been obtained by different methods of observation at the different stations. Furthermore, the observations refer to different hours of the day.

The drift of the amplitude pattern at Tromsø is mainly towards the east and south-west. The distribution of the observed drift directions is given in Fig. (8). If we neglect a minor southerly component, the drift of the amplitude pattern of the sporadic  $E$  echo is almost parallel to the auroral zone. Fig. (8) shows that more than 80 % of the observed drift velocities has a southerly component. The mean drift is towards the west before local midnight and towards the east after midnight (Vide Fig. (2)).

The movement of irregularities in the auroral ionosphere has been studied by a large number of workers using very high frequencies. Observations of this kind indicate

that field-aligned irregularities are present in the ionosphere (LEADABRAND et al [17]). These irregularities drift towards west before midnight and towards east after midnight (BULLOUGH and KAISER [18]), in fair agreement with our results. The mean drift speed deduced by these authors is, however, as high as 1000–2000 m sec<sup>-1</sup>.

**5. Sporadic E drift and magnetic activity.** The geomagnetic storms in the auroral zone are usually ascribed to enhanced current density in the quasi-zonal current systems between 100 and 150 km (FUKUSHIMA [19]). This enhancement is probably caused by two effects: (i) an increased electron density at these heights and /or (ii) an increased, external electric field. The well-known positive correlation between the magnetic activity and the critical frequency of the sporadic *E* layer (SMITH [20]) indicates that the electron density in the region in question is increased during magnetic storms. However, no method seems to be available at present by which the variations in the electric field at these altitudes may be measured directly.

The relation between the drifts in the sporadic *E* layer above Tromsø and the geomagnetic activity has been studied. The horizontal component ( $\Delta H$ ) of the magnetic storm vector (KROGNESS et al [21]) observed at Tromsø is used as a parameter for the geomagnetic activity. This parameter is a function of the flux of charged particles across the meridian plane through the station. For westerly currents  $\Delta H$  is negative, for easterly currents  $\Delta H$  is positive.

Results from the study are given in Fig. (9), in which the zonal component of the drift velocity ( $V_s$ ) in the sporadic *E* layer is plotted versus the observed value of  $\Delta H$ . The sporadic *E* layer drift is mainly towards the east during negative storms, and towards the west during positive storms. Furthermore, the easterly drift increases with increasing value of  $\Delta H$ . A certain phase difference between  $\Delta H$  and  $V_s$  may be inferred from Fig. (9). Thus  $V_s$  has a westerly component of the order of 100–200 m sec<sup>-1</sup> during hours when  $\Delta H$  vanishes. It is important to note that the speed of rotation of the earth at 70° N is approximately 160 m sec<sup>-1</sup>. Fig. (9) therefore seems to indicate that the mean velocity of the irregularities in the auroral *E*<sub>s</sub> region is practically zero (referred to a non-rotating earth) during hours when  $\Delta H$  vanishes.

The correspondance between the moving irregularities in the auroral zone and the geomagnetic storm current systems has been studied by a large number of workers. (A summary of results has recently been given by NICHOLS [22]). HEPPNER [23] has pointed out that negative magnetic storms are associated with eastward drifts of visual auroras. The drift of the irregularities in the auroral ionosphere associated with the "auroral backscatter" on very high frequencies is also towards the east during hours when the horizontal component of the magnetic storm vector is negative, shifting to a westerly when  $\Delta H$  becomes positive (BULLOUGH et al. [24]). There seems therefore to be good consistency between the phase of the storm current and the drift direction of the sporadic *E* layer, of the visual aurora and of the irregularities which give rise to the scatter echoes on very high frequencies.

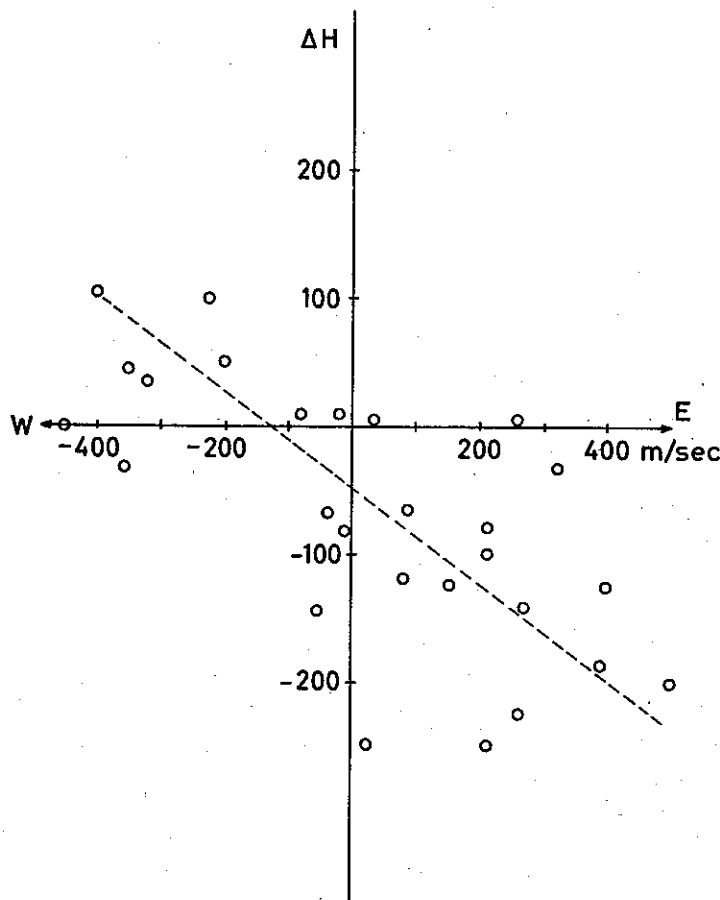


Fig. 9. Zonal component of the drift velocity in the  $E_s$  layer plotted versus the horizontal component of the geomagnetic storm vector.

**6. Discussion of the observational results.** The observations of the sporadic  $E$  layer in the auroral ionosphere reported in the present paper introduce a number of theoretical problems. At present these problems may only be the subject of speculations; partly because the number of observations available is very limited, partly because the physical processes involved, such as the sources of ionization and the dynamics of the irregularities, are not well known.

It may, however, be of importance to discuss some of the observations in a semi-quantitative way. In this section the following two problems will be treated:

- 1) The observed anisotropy in the  $E_s$  amplitude pattern
- 2) The drift of the amplitude pattern, and its relation to the geomagnetic storm current systems.

**6.1. Structure of the sporadic  $E$  region.** In the previous sections only the statistical properties of the amplitude pattern of the sporadic  $E$  echo have been discussed. In the following discussion it is assumed that the horizontal projection of the irregularities in the sporadic  $E$  layer is conformal to the amplitude pattern of the echo.

As the geomagnetic lines of force are nearly perpendicular to the earth's surface at Tromsø, the horizontal projection of the irregularities is approximately equal to the projection on to a plane normal to the field lines. It has been shown by LEADABRAND et al. [17] that field-aligned irregularities in the ionization exist within the auroral ionosphere. The present study indicates that the irregularities are field-aligned "sheets" of ionization rather than columns with circular cross-sections. Possible theories for the formation of such irregularities will be discussed in the two subsequent sections.

The electron density distribution in the ionosphere is controlled by three processes: (i) production of free electrons by incoming energy, mainly of solar origin, (ii) disappearance of free electrons by attachment and recombination, and (iii) redistribution of existing ionization by convection, accumulation and diffusion. The time variations of the electron density  $n$  is therefore given by the following equation:

$$\frac{\partial n}{\partial t} = -\alpha n^2 - \beta n - \nabla \cdot (\vec{V} n) + q \quad (6.1)$$

where  $q$  is the rate of production due to external sources.  $\alpha$  and  $\beta$  are the recombination and attachment coefficient, respectively, and  $\vec{V}$  the velocity of the electrons.

In the following two sub-sections the different terms of the equation (6.1) will be discussed as possible contributors to the formation of the anisometric irregularities. As obviously a decay process due to recombination and attachment cannot introduce any anisometric effects in the sporadic  $E$  layer, the discussion will be limited to the last two terms.

**a. Diffusive processes.** The ionization of the sporadic  $E$  layer in the auroral zone is known to possess a "cloudy structure". Due to regular and irregular motions of the electrons, the shape of the "clouds" change rapidly. The deformation of a spherical "cloud" of ionization under the action of nonisotropic diffusion will briefly be discussed in this section.

The velocity of an electron in the presence of an external electric field  $\vec{E}$  normal to  $\vec{B}$  is given by equation (6.2), if the inertial and gravitational forces are neglected.

$$\vec{V} = M_e (e\vec{E} + kT \frac{\nabla n}{n}) = \vec{V}_E + \vec{V}_p \quad (6.2)$$

$M_e$  being the mobility tensor,  $k$  Boltzman's constant and  $T$  the temperature. If the  $z$ -axis is chosen to be parallel to the earth's magnetic field, the mobility tensor reduces to a simple function of the Pedersen mobility  $t_e$ , the Hall mobility  $h_e$  and the longitudinal mobility  $l_e$ :

$$M_e = \begin{pmatrix} -t_e & h_e & 0 \\ -h_e & -t_e & 0 \\ 0 & 0 & -l_e \end{pmatrix} \quad (6.3)$$

The divergence term in equation (6.1) may therefore be written: (if  $T$  is assumed to be constant):

$$\begin{aligned} \Delta \cdot (\vec{V}n) = \vec{V}_E \cdot \nabla n - nt_e \nabla \cdot \vec{E} + n(t_e - l_e) \frac{\partial E_z}{\partial z} + nh_e (\nabla \times \vec{E}) \cdot \vec{e}_3 - \\ - kTt_e \nabla^2 n - kT(l_e - t_e) \frac{\partial^2 n}{\partial z^2} \end{aligned} \quad (6.4)$$

$\vec{e}_3$  being the unity vector in the direction of the  $z$ -axis. If the external electric field changes sufficiently slowly throughout the medium, the first term on the right side corresponds to a bodily movement of the cloud. The next three terms correspond to decay processes caused by spatial variations in the external field. It has been shown (CLEMMOW and JOHNSON [25]) that the decay processes associated with an external, electric field are of less importance in the  $E$  region than the diffusive decay. Equation (6.4) therefore reduces to:

$$\nabla \cdot (\vec{V}n) \approx \vec{V}_E \cdot \nabla n - kTt_e \nabla^2 n - kT(l_e - t_e) \frac{\partial^2 n}{\partial z^2} \quad (6.5)$$

At the 100 km level the ratio  $l_e/t_e$  is approximately 100, if the positive ions are assumed to be at rest (MAEDA [26]).

Thus, according to equation (6.5), the diffusion takes place much more rapidly along the field lines than normal to these. A spherical cloud of ionization will, under the action of diffusion, be deformed to a field-aligned irregularity with a circular cross-section. Diffusive processes may therefore produce field-aligned irregularities with circular cross-sections, provided the "time constant" of the diffusion is much less than the "life time" of the irregularity.

In the  $F_2$ -layer the decay of free electrons by recombination and attachment is rather slow, and it has been suggested that the field-aligned irregularities in this layer may be formed by diffusion (SPENCER [27]). Field-aligned irregularities observed in other ionospheric regions (LEADABRAND et al [17], HARANG and PEDERSEN [12] and UNWIN [23]) may possibly also be ascribed to the same effect. It seems improbable, however, from equation (6.5) that irregularities with non-circular cross-sections may be formed by anisotropic diffusion.

**b. The source of ionization.** The close relationship between the sporadic  $E$  ionization, the occurrence of visual aurora and the magnetic storminess is well established (KNECHT [29], OMHOLT [30] and HEPPNER [23]). It has therefore been suggested that the sporadic  $E$  ionization in the auroral zone is formed by charged particles of solar origin (SMITH [20]). The nature of the incoming solar corpuscles has been discussed by a large number of workers, and a survey of results has recently been given by PARKER [31]. The main constituents of the incoming particle stream are protons and electrons. As the stream invades the earth's magnetic field, some of the particles are captured by the field (STØRMER [32]). These particles will then start

spiralling around the magnetic lines of force, and oscillate between a northern and a southern mirror-point. Furthermore, as the earth's magnetic field is non-homogeneous, the electrons tend to drift slowly towards east and the protons towards west (ALFVÉN [33]).

A corpuscle captured by the earth's magnetic field will thus be confined to one of the surfaces described when the magnetic field lines are rotated around the earth's magnetic axis. Let  $R$  and  $\lambda$  be the polar coordinates of the surface in a geomagnetical meridional plane. Then, for the dipole assumption:

$$R = R_e \cos^2 \lambda \quad (6.6)$$

$R_e$  being the geocentric distance of the surface at the geomagnetical equator.

A particle captured by the earth's magnetic field is not allowed to move from one of the surfaces given by equation (6.6) to another. Hence  $R_e$  is a conservative parameter for the particle:

$$\frac{dR_e}{dt} \approx 0 \quad (6.7)$$

An experimental proof for the validity of equation (6.7) has been obtained during the experiment "Argus" [34].

One may introduce the "thickness" of one trapping surface as the diameter of the gyrocircle:

$$D = 2\rho = 2 \frac{cv_\perp}{eB} \quad (6.8)$$

The particles trapped in a certain shell given by equation (6.6) may penetrate into the lower atmosphere at high latitudes and produce ionization in an area which is unlimited in the east/west direction, whereas the north/south extent of the area should be comparable with  $D$ . It therefore seems reasonable that ionospheric layers formed by trapped particles are more uniform in an east/west direction than in the north/south direction, which is in accordance with our observations of the sporadic  $E$  layer in the auroral zone.

At present this model cannot be tested quantitatively, as the energy distribution of the trapped particles is unknown. It has been suggested by McILWAIN [35] that electrons in the energy range 10–20 keV play an important role in the formation of active, visual aurora. The gyroradius near the mirror point of such particles is approximately 8–10 m corresponding to a diameter equal to 15–20 m. This distance is somewhat smaller than the meridional "scale of structure" in the sporadic  $E$  layer, which is 80–160 m.

**6.2 Drift of the amplitude pattern of the Es-echo.** There seems to be at least three possible explanations for the observed drift of the amplitude pattern of the sporadic  $E$  echo:

- 1) Horizontal movements of clouds of ionization caused by horizontal wind systems. (The term "wind" refers to movement of unionized matter).
- 2) Horizontal movements caused by an external electric field.
- 3) Motion of a non-uniform source of ionization.

The connection between the ionospheric winds and the movements of the ionospheric irregularities has been studied by different authors. Due to the high collision frequency in the  $E_s$  region, a wind may be of great importance in the horizontal displacements of ionization (RATCLIFFE [36]). As, however, the sound velocity at the altitudes in question is of the order  $300 \text{ m sec}^{-1}$ , (based upon values given by HAVENS et al. [37]), it seems doubtful that the highest drift velocities observed may be ascribed to winds. In fact, observations of meteor-trails clearly show that the wind speed is much lower in the auroral  $E$  region than the highest drift speeds observed.

The movement of irregularities in an ionized gas in the presence of electric and magnetic fields is still an unsolved problem. The particular case when the irregularities are elongated along the magnetic field lines has been the subject of theoretical studies by MARTYN [38] and CLEMMOW, JOHNSON and WEEKES [39]. The velocity of a weak, field-aligned irregularity in the presence of an external electric field  $\vec{E}$  is given by (CLEMMOW and JOHNSON [25]):

$$\vec{V} = \frac{\vec{E} \times \vec{B}}{\left(1 + \frac{\nu_e \nu_i}{\omega_e \omega_i}\right) B^2} \quad (6.9)$$

$\nu_i$  and  $\nu_e$  being the collision frequency for ions and electrons, respectively, and  $\omega_i$  and  $\omega_e$  the corresponding gyro frequencies. At the 100 km level  $\nu_i = 9 \cdot 10^3 \text{ sec}^{-1}$  and  $\nu_e = 2 \cdot 10^5 \text{ sec}^{-1}$  (MAEDA [26]). If  $B$  is assumed to be equal to  $4 \cdot 10^{-5} \text{ Wb/m}$ ,  $\omega_e = 7 \cdot 10^6 \text{ sec}^{-1}$  and  $\omega_i = 1.6 \cdot 10^2 \text{ sec}^{-1}$ , then:

$$V = 10^4 E \quad (6.10)$$

The electric field required to produce a drift speed of  $750 \text{ m sec}^{-1}$  (the highest drift speed observed in the  $E_s$  region above Tromsø) is thus  $70\text{--}80 \text{ mV m}^{-1}$ . As the actual shape of the irregularities in the sporadic  $E$  region is unknown, it is not clear whether equation (6.10), which strictly holds only for field-aligned irregularities, is valid for this actual case. There is, however, a remarkable consistency between this field strength and the storm field deduced from the Chapman and Ferraro ring current (MARTYN [40]), the latter being of the order  $100 \text{ mV m}^{-1}$ .

An alternative explanation for the observed drift is that the source of ionization has an apparent horizontal movement. As, however, the "life-time" of the irregularities in the  $E_s$  region is as high as 10–20 minutes, it seems improbable that this may explain the observed variations in the echo amplitude with periods less than one second. This conclusion is confirmed by results from studies of scatter irregularities in the auroral zone using VHF (BOWLES [41]).



**7. Conclusions.** The results from a study of the small-scale irregularities in the amplitude pattern of the night-time sporadic *E* echo in the auroral zone, given in the present paper, may be summarized as follows:

- 1) The irregularities are elongated in an east/west direction, and the mean axis ratio in the correlation ellipses is 3:1.
- 2) The mean horizontal extent of the irregularities is approximately 250 m (along the minor axis of the correlation ellipses).
- 3) The irregularities in the amplitude pattern are found to move nearly parallel to the visual auroral zone.
- 4) The mean drift speed of the amplitude pattern is  $280 \text{ m sec}^{-1}$ . Drift velocities up to  $1460 \text{ m sec}^{-1}$  have been observed.
- 5) The drift is towards the west during positive magnetic storms, and towards the east during negative storms, and the drift velocity is somewhat higher during magnetic storms than during quiet conditions. During hours when the magnetic storm vector is zero, the drift motion relative to a non-rotating earth practically vanishes.

The observations have been briefly discussed. It has been assumed that the fading of the *E<sub>s</sub>* echo is caused by field-aligned irregularities, having elliptical "cross-sections". Hence the irregularities are field-aligned "sheets" of ionization rather than columns with circular "cross-sections". It has been shown that such irregularities cannot be formed by diffusive redistribution of existing ionization. The shape of the irregularities may qualitatively be explained if the ionizing particles are trapped in the earth's magnetic field.

The drift speeds of the irregularities in the sporadic *E* region are assumed to be 50% of the drift speeds of the amplitude patterns. It is obvious that the highest velocities observed cannot be equivalent to the wind velocities at the same altitude. In order to explain the highest velocities observed, it seems necessary to postulate the existence of an external, meridional electric field. The magnitude of this field is deduced as a function of the drift velocity under certain simplifying assumptions. The field corresponding to the highest drift velocities observed is of the order  $80 \text{ mV m}^{-1}$ .

**Acknowledgement.** The author would like to express his gratitude to Professor L. HARANG and Dr. B. LANDMARK for encouragement and suggestions. He is also grateful to the staff of the Auroral Observatory at Tromsø for assistance during the observations. His gratitude is extended to the author's colleagues at the *NDRE* for stimulating discussions. The work was supported by the *EO-ARDC* under contract *AF 61(052)–228*.

## APPENDIX

The "Cambridge method" for deducing the correlation properties of the amplitude pattern of the ionosphere echoes. The structure and drift of the amplitude pattern of a signal reflected from an ionosphere layer may be deduced if the time variation of the signal is known at three points over the ground. The method [8—11] is based upon three assumptions:

- 1) Curves of constant spatial autocorrelation for the pattern are concentric, conformal ellipses.
- 2) The amplitude pattern changes very slowly as it moves.
- 3) The temporal autocorrelation function is conformal to the spatial, "one-dimensional" autocorrelation function.

Let the combined temporal and spatial autocorrelation function of the amplitude pattern be given in polar coordinates by:

$$\rho = \rho(r, \varphi, \tau) \quad (\text{A1})$$

By recording the time variation of the echo amplitude at the three points:  $(r, \varphi) = (0, 0)$ ,  $(a, 0)$  and  $(a, \frac{\pi}{2})$ , the following spatial correlation functions may be deduced:

$$\rho_{01} = \rho(a, 0, \tau) \quad (\text{A2})$$

$$\rho_{10} = \rho(a, \frac{\pi}{2}, \tau)$$

$$\rho_{11} = \rho(a, \frac{3\pi}{4}, \tau)$$

$$\rho_{\tau} = \rho(0, 0, \tau)$$

From assumption 1 follows:

$$\rho(r, \varphi, 0) = \rho(r(\varphi), 0) \quad (\text{A3})$$

and a "correlation ellipse" is given by:

$$r(\varphi) = A(\rho) (1 + (\Gamma^2 - 1) \sin^2(\varphi - \psi))^{-1/2} \quad (\text{A4})$$

where  $A$  is the major semiaxis in the correlation ellipse,  $\Gamma$  the axis ratio ( $\Gamma > 1$ ) and  $\psi$  the angle between the  $x$ -axis and the major axis of the correlation ellipse.

From assumption 3:

$$\rho\left(\frac{r(\varphi)}{V_c(\varphi)}, 0\right) = \rho(0, \tau) \quad (\text{A5})$$

The parameter  $V_c(\varphi)$ , having the dimension of velocity, is usually called the "fading velocity". It may be shown that the fading velocity is a function of the non-systematical drifts in the amplitude pattern.

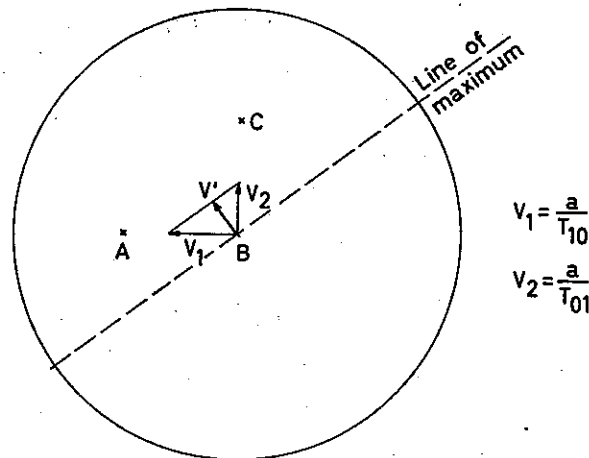


Fig. A1. Drift of an isometric amplitude pattern.

The drift velocity of a bodily moving isometric amplitude pattern ( $V_c(\varphi) = \text{constant}$ ) may easily be deduced when the mean time shifts ( $T_{01}, T_{10}, T_{11}$ ) between similar fades at the three antennas are known (Fig. (A1)).

For an anisometric amplitude pattern, however, it is essential to know the form and orientation of the correlation ellipses in order to deduce the drift velocity  $V'$ .

The "apparent" drift velocity  $V_T$  deduced from time shifts between "similar fades" is normal to the so-called "maximum line" in the correlation ellipses. It may be shown

that the "maximum line" and the direction of the drift  $V'$  are conjugated diameters in the ellipses. Furthermore,  $V' = V_T \cdot \sec \varphi$  (Fig. (A2)). Thus the drift velocity of an anisometric, bodily drifting amplitude pattern may be deduced if the apparent drift velocity and the "correlation ellipses" of the pattern are known.

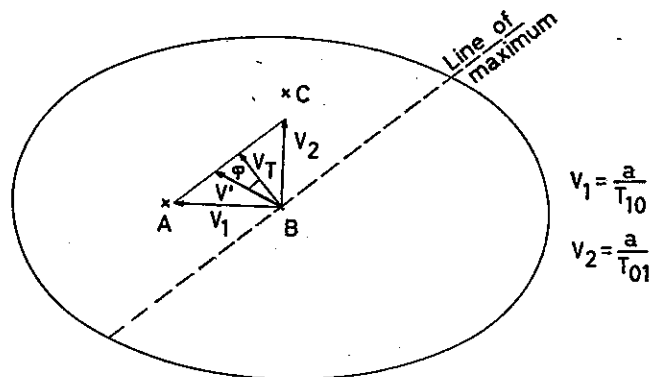


Fig. A2. Drift of an anisometric amplitude pattern.

When non-systematical drifts occur in the amplitude pattern, the term "true drift" has no meaning. In this case the true drift velocity is defined as "the velocity of an observer who has so adjusted his motion over the ground that he experiences the slowest possible speed of fading" (BRIGGS et al. [10]).

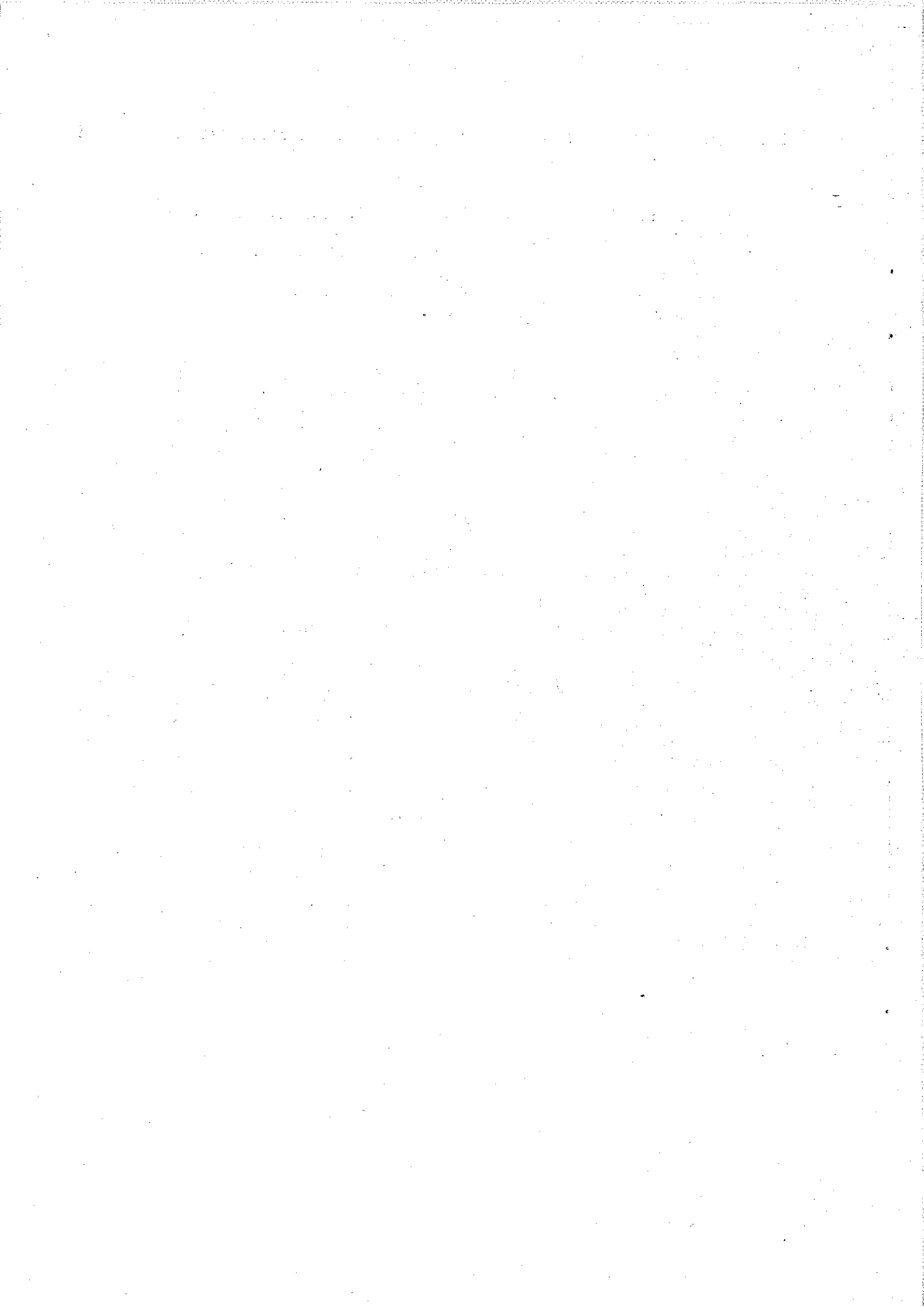
It has been shown [11] that the "true drift"  $\vec{V}$  is parallel to the drift  $\vec{V}'$ , which is deduced by the procedure given above. The "true" speed of the amplitude pattern is easily deduced by equation (A6) [11], in which  $V_c(\varphi_1)$  is the "fading velocity" in a direction parallel to  $\vec{V}'$ .

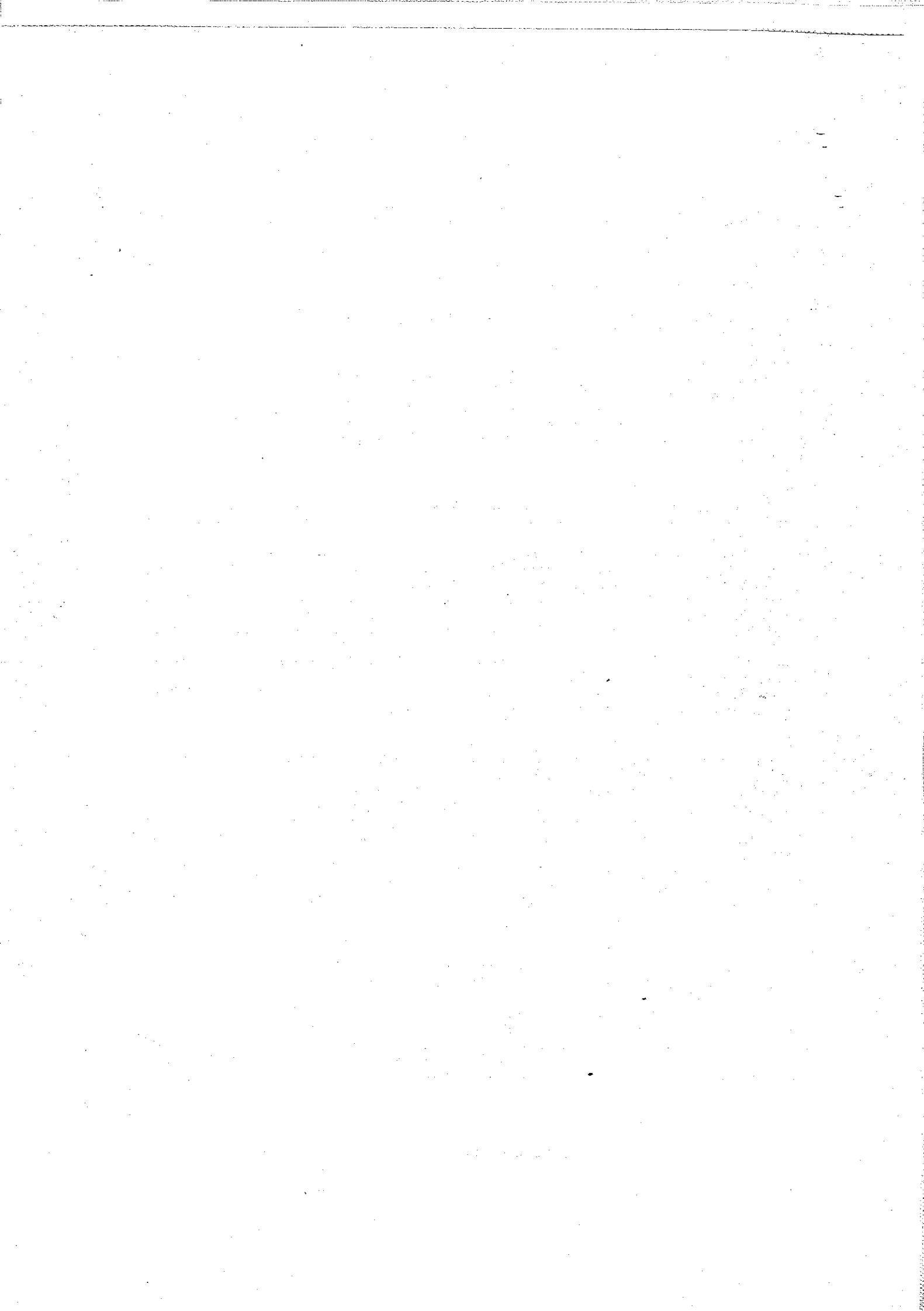
$$\vec{V} = \left( \frac{V_c(\varphi_1)}{V'} \right)^2 \vec{V}' \quad (\text{A6})$$

This equation shows that for a bodily drifting amplitude pattern ( $\vec{V} = \vec{V}'$ ) the "fading velocity" in the drift direction is equal to  $\vec{V}'$ .

## REFERENCES

- 1 GERSON, N. C.: *Geofis. pura e appl.*, **18**, 3 (1950). *Canad. J. Phys.*, **29**, 251 (1951).
- 2 RAWER, K.: *Geofis. pura e appl.*, **32**, 170 (1955).
- 3 OKSMAN, J. O., and S. A. BOWHILL: *Sci. Rep. No. 132*, Penn. State Univ. (1960).
- 4 MÆHLUM, B.: *Geofys. Publ.*, **23**, No 1 (1962).
- 5 HAGG, E. L., and G. H. HANSSON: *Canad. J. Phys.*, **32**, 790 (1954).
- 6 BRIGGS, H. B.: *AGARDograph*, **34**, 169 (1958).
- 7 WRIGHT, R. W. H.: Private communication.
- 8 MITRA, S. N.: *Inst. Electr. Engrs.*, **96**, 441 (1949).
- 9 BOOKER, H. G., J. A. RATCLIFFE, and D. H. SHINN: *Phil. Trans., Roy. Soc. London*, **A242**, 579 (1950).
- 10 BRIGGS, B. H., G. J. PHILLIPS, and D. H. SHINN: *Proc. Phys. Soc.*, **B 63**, 106 (1950).
- 11 PHILLIPS, G. J., and M. SPENCER: *Proc. Phys. Soc.* **B 68**, 481 (1955).
- 12 HARANG, L., and K. PEDERSEN: *Geofys. Publ.*, **19**, No. 10 (1956).
- 13 FINDLAY, J. W.: *J. Atmosph. Terr. Phys.*, **3**, 73 (1953).
- 14 THOMAS, J. A., and M. J. BURKE: *Austr. J. Phys.*, **9**, 440 (1956).
- 15 HARVEY, J. A.: *Austr. J. Phys.*, **8**, 523 (1955).
- 16 MEEK, J. H.: *J. Geophys. Res.*, **54**, 339 (1949).
- 17 LEADABRAND, R. L., L. DOLPHIN, and A. M. PETERSON: *Final Rep., Contract No. AF 30 (602) -1462*. Stanford Res. Inst. (1957).
- 18 BULLOUGH, K., and T. R. KAISER: *J. Atmosph. Terr. Phys.*, **5**, 189 (1954).
- 19 FUKUSHIMA, N.: *J. Fac. Sci., Univ. Tokyo*, **8**, 291 (1953).
- 20 SMITH, E. K.: *N.S.B. Circular 582* (1957).
- 21 HARANG, L., O. KROGNESS, and E. TØNSBERG: *Publ. Norske Inst. Kosmisk Fysikk*. No. 2 (1933).
- 22 NICHOLS, B.: *Proc. I.R.E.*, **47**, 245 (1959).
- 23 HEPPNER, J. P.: *Thesis Calif. Inst. of Technology*, Pasadena (1945).
- 24 BULLOUGH, K., T. W. DAVIDSON, and C. D. WATKINS: *J. Atmosph. Terr. Phys.*, **11**, 237 (1957).
- 25 CLEMMOW, P. C., and M. A. JOHNSON: *J. Atmosph. Terr. Phys.*, **16**, 21 (1959).
- 26 MAEDA, H.: *Geomag. and Geoele.*, **3**, 94 (1953).
- 27 SPENCER, M.: *Proc. Phys. Soc.*, **B 68**, 493 (1955).
- 28 UNWIN, R. W.: *J. Geophys. Res.*, **63**, 501, (1958).
- 29 KNECHT, R. W.: *J. Geophys. Res.*, **61**, 59 (1956).
- 30 OMHOLT, A.: *J. Atmosph. Terr. Phys.*, **7**, 73 (1955).
- 31 PARKER, E. N.: *Proc. I.R.E.*, **47**, 239 (1959).
- 32 STØRMER, C.: *The Polar Aurora*, Oxford (1955).
- 33 ALFVÉN, H.: *Kungl. Svenska Vetenskapsakad. Handl.*, **18**, No. 3 (1939) and No. 9 (1940).
- 34 VAN ALLEN, J. A., C. E. MC ILWAIN, and G. H. LUDWIG: *J. Geophys. Res.*, **64**, 877 (1959).
- 35 MC ILWAIN, C. E.: *Dept. of Phys. and Astron., State Univ. Iowa, (SUI 59-29)*, (1959).
- 36 RATCLIFFE, J. A.: *J. Geophys. Res.*, **64**, 2102 (1959).
- 37 HAVENS, R. J., R. T. KOLL, and H. E. LAGOW: *J. Geophys. Res.* **57**, 59 (1952).
- 38 MARTYN, D. F.: *Phil. Trans., Roy. Soc. London*, **A 246**, 306 (1953).
- 39 CLEMMOW, P. C., M. A. JOHNSON, and K. WEEKES: *The Physics of the Ionosphere*, Phys. Soc. London, p. 136 (1954).
- 40 MARTYN, D. F.: *Nature*, **167**, 92 (1951).
- 41 BOWLES, K. L.: *Thesis, Cornell Res. Rep. EE 248* (1955).





Avhandlinger som ønskes opptatt i «Geofysiske Publikasjoner», må fremlegges i Videnskaps-Akademiet av et sakkyndig medlem.

**Vol. XX.**

- No. 1. B. J. Birkeland: Homogenisering der Temperaturreihe Greenwich 1763—1840. 1957.  
» 2. Enok Palm: On Reynolds stress, turbulent diffusion and the velocity profile in stratified fluid. 1958.  
» 3. Enok Palm: Two-dimensional and three-dimensional mountain waves. 1958.  
» 4. L. Vegard: Recent progress relating to the study of aurorae and kindred phenomena. 1958.  
» 5. Leiv Harang: Height distribution of the red auroral line in polar aurorae. 1958.  
» 6. Bernt Mæhlum: The diurnal- and sunspot-cycle variation of the layers *E*, *F1* and *F2* of the ionosphere as observed in Norway during the period 1932—1956. 1958.  
» 7. Jonas Ekman Fjeldstad: Ocean current as an initial problem. 1958.  
» 8. Olav Holt and Bjørn Landmark: Some statistical properties of the signal fine structure in ionospheric scatter propagation. 1958.  
» 9. L. Vegard, S. Berger, and A. Nundal: Results of auroral observations at Tromsø and Oslo from the four winters 1953—54 to 1956—57. 1958.  
» 10. Eigil Hesstvedt: Mother of pearl clouds in Norway 1959.  
» 11. A. Omholt: Studies on the excitation of aurora borealis. I. The hydrogen lines. 1959.  
» 12. G. Kvifte: Nightglow observations at Ås during the I. G. Y. 1959.  
» 13. Odd H. Sælen: Studies in the Norwegian Atlantic current. Part I: The Sognefjord section. 1959.

**Vol. XXI.**

- No. 1. A. Omholt: Studies on the excitation of aurora borealis II. The forbidden oxygen lines. 1959.  
» 2. Tor Hagfors: Investigation of the scattering of radio waves at metric wavelengths in the lower ionosphere. 1959.  
» 3. Håkon Mosby: Deep water in the Norwegian Sea. 1959.  
» 4. Søren H. H. Larsen: On the scattering of ultraviolet solar radiation in the atmosphere with the ozone absorption considered. 1959.  
» 5. Søren H. H. Larsen: Measurements of atmospheric ozone at Spitsbergen (78°N) and Tromsø (70°N) during the winter season. 1959.  
» 6. Enok Palm and Arne Foldvik: Contribution to the theory of two-dimensional mountain waves 1960.  
» 7. Kaare Pedersen and Marius Todsen: Some measurements of the micro-structure of fog and stratus-clouds in the Oslo area. 1960.  
» 8. Kaare Pedersen: An experiment in numerical prediction of the 500 mb wind field. 1960.  
» 9. Eigil Hesstvedt: On the physics of mother of pearl clouds. 1960.

**Vol. XXII.**

- No. 1. L. Harang and K. Malmjord: Drift measurements of the E-layer at Kjeller and Tromsø during the international geophysical year 1957—58. 1960.  
» 2. Leiv Harang and Anders Omholt: Luminosity curves of high aurorae. 1960.  
» 3. Arnt Eliassen and Enok Palm: On the transfer of energy in stationary mountain waves. 1961.  
» 4. Yngvar Gotaas: Mother of pearl clouds over Southern Norway, February 21, 1959. 1961.  
» 5. H. Økland: An experiment in numerical integration of the barotropic equation by a quasi-Lagrangian method. 1962.  
» 6. L. Vegard: Auroral investigations during the winter seasons 1957/58—1959/60 and their bearing on solar terrestrial relationships. 1961.  
» 7. Gunnvald Bøyum: A study of evaporation and heat exchange between the sea surface and the atmosphere. 1962.

**Vol. XXIII.**

- No. 1. Bernt Mæhlum: The sporadic E auroral zone. 1962.  
» 2. Bernt Mæhlum: Small scale structure and drift in the sporadic E layer as observed in the auroral zone. 1962.  
» 3. L. Harang and K. Malmjord: Determination of drift movements of the ionosphere at high latitudes from radio star scintillations. 1962.  
» 4. Eyvind Riis: The stability of Couette-flow in non-stratified and stratified viscous fluids. 1962.  
» 5. E. Frogner: Temperature changes on a large scale in the arctic winter stratosphere and their probable effects on the tropospheric circulation. 1962.